Composites: Part A 100 (2017) 161–169

Contents lists available at ScienceDirect

Composites: Part A

journal homepage: www.elsevier.com/locate/compositesa

High strain-rate dynamic mechanical properties of Kevlar fabrics impregnated with shear thickening fluid

Saisai Cao [a], Qian Chen [a], Yunpeng Wang [a], Shouhu Xuan [a,*], Wanquan Jiang [b], Xinglong Gong [a,*]

[a] CAS Key Laboratory of Mechanical Behavior and Design of Materials, Department of Modern Mechanics, University of Science and Technology of China (USTC), Hefei 230027, PR China
[b] Department of Chemistry, USTC, Hefei 230026, PR China

ARTICLE INFO

Article history:
Received 18 January 2017
Received in revised form 27 March 2017
Accepted 20 April 2017
Available online 22 April 2017

Keywords:
A. Fabrics/textiles
A. Nanoparticles
B. Impact behavior
D. Mechanical testing
Shear thickening fluid

ABSTRACT

To investigate the anti-impact mechanism, the mechanical property and energy absorption of the STF impregnated Kevlar (STF/Kevlar) fabric at high strain rate were conducted using a split Hopkinson pressure bar (SHPB) system. The volume fraction of STF, number of fabric specimens, and impact velocity highly affected the dynamic mechanical performance of the STF/Kevlar composite. The energy transfer rate decreased from 0.85 to 0.01 once the number of fabric specimens increased from 2 layers to 8 layers. The strain rate stiffening mechanism of the STF/Kevlar was analyzed. The Kevlar fabrics underwent four sections during the impact process. The STF was mainly worked in the slip and deformation section by enhancing the friction between fabric yarns and preventing the fabric yarns from slipping. Overall, this work demonstrated that the multilayer Kevlar fabrics impregnated with high volume fraction of STF were the optimal choice for soft body armor.

1. Introduction

Body armors are designed to protect soldiers from the damage caused by bullets and other weapons. The traditional body armors are made of ceramics and metal, which makes the body armors bulky. To improve the flexibility and reduce the weight of the body armors, high strength and energy absorption fabrics such as Kevlar, Twaron and Spectra have been developed for the soft body armors [1–3]. Usually, almost 20–50 layers of fabrics are required to satisfy the bulletproof requirements. As a result, the comfort of the body armors sharply decreases. Therefore, besides the ballistic requirement, the low weight and high flexibility become the critical points for body armors. Recent years, shear thickening fluid (STF) has got more and more attention due to its unique shear thickening property. As a type of non-newton fluid, the viscosity of STF increases dramatically when the shear rate exceeds a critical value. After easing the applied shear rate, the STF can recover from solid like state to the initial fluid state [4–8]. The shear thickening property is expected to enhance the ballistic performance of fabrics. Therefore, the STF incorporated Kevlar has been proven to be an ideal body armor because of its low density [9–15].

In the early days, a lot of researches were conducted on the stab resistance of STF impregnated (STF-treated) fabric composite [9–20]. Decker et al. [9] investigated the stab resistance of STF-treated Kevlar and nylon fabrics. It was found that the STF-treated fabric exhibited significant improvements in puncture resistance while a slight enhancement in cut protection. Feng et al. [15] prepared different STFs based on the fumed silica and submicron silica particles. After incorporating these STFs into the Kevlar fabrics, the quasi-static stab resistance properties were studied. The force-displacement curve and the microstructure diagram demonstrated that the properties of particles influenced the stab resistance properties of fabrics. Moreover, it was reported the STFs also highly affected the friction between fabric yarns [17,21–24]. Gong et al. [17] found that the pull-out force of the Kevlar/STF fabrics was much larger than the neat fabric. Typically, the pull-out force of the Kevlar/STF fabrics increased with the pull-out speed, which was consistent with the shear thickening property of STFs. Meanwhile, lots of investigations on the ballistic properties of the composite have been reported [18,25–29]. Park et al. [28] focused on the energy absorption of STF-treated fabric composite under high speed (>700 m/s) impact and studied the change of energy absorption value with the impact velocity by changing the number of Kevlar layers and area density.

The mechanical properties of the STF/fabric composite have got more and more attention since their importance for application [15,30,31]. Lu et al. [30] studied the quasi-static and low-velocity impact compressive behavior of the warp-knitted spacer fabrics (WKSF) impregnated with STF. The compressive behavior of the

* Corresponding author.
E-mail addresses: xuansh@ustc.edu.cn (S. Xuan), gongxl@ustc.edu.cn (X. Gong).

http://dx.doi.org/10.1016/j.compositesa.2017.04.015
1359-835X/

STF/WKSF had a significant strain rate effect. In comparison to the neat WKSF, the STF/WKSF showed a higher energy absorption and a lower peak load. Haris et al. [31] studied the STF/Twaron fabrics with a shock tube device and ballistic tests. The results showed that the STF-treated fabrics could be applied in both ballistic protection and shock wave mitigation. By using uniaxial tensile, bias-extension, and picture-frame tests, Na et al. [32] investigated the rate-dependent behavior of an STF-im-AR fabric. Although the STF effect was not evident in the tensile properties, the shear resistance of the fabric was enhanced significantly. To further investigate the enhancing mechanism, Lu et al. [33] and Park et al. [34] also established a numerical simulation model to explain the energy absorption of the composite at the viewpoint of friction. Lee and Kim [35] performed a computational analysis to consider the effect of STF impregnation on the ballistic performance of STF impregnated fabrics. The results showed that the increased friction induced by STF impregnation encouraged a greater interaction between yarns that allowed the fabric to maintain its woven structure longer than neat fabric during the impact process.

The split Hopkinson pressure bar (SHPB) system is widely used to test the mechanical properties of materials at high strain rates varying from $10^2\ s^{-1}$ to $10^4\ s^{-1}$ [36–43]. A stress pulse is generated while the striker bar hits the incident bar. Then the specimen is deformed by the stress pulse. Finally, the stress-strain curve of the specimen can be obtained from the waveforms before and after the specimen. Up to now, the researches on the bullet-proof fabrics impregnated with STF are mainly in the stab resistance and ballistic resistance aspects. However, the high strain rate dynamic property of the STF strengthened fabrics has not been reported till now. The body armor was originally used to prevent the bullet through the body. However, the liver, heart, spleen, and spinal cord were still vulnerable to injury despite of the use of soft body armor [44–46]. As we know, stress waves are generated while the high-speed bullet hits body armor, where the energy of the stress pulse is quite considerable and even deadly. Stress waves in tissue may result in very high local forces, producing small but very rapid distortions of tissue (strain), which causes non penetrating trauma (NPT) [45]. Therefore, it is essential to investigate the dissipation of strain energy and dynamic mechanical properties of the bullet-proof fabrics impregnated with STF under impact.

In this work, the high strain-rate mechanical property of the STF/Kevlar was studied by using SHPB system. Firstly, as a comparison, the stab resistance performance of the STF/Kevlar composites was tested by a drop tower. A knife impactor and a spike impactor were chosen according to the National Institute of Justice (NIJ) standard for stab testing of protective armors (NIJ 0115.00, 2000). Then, an SHPB system was used to test the mechanical properties and energy absorption of the STF/Kevlar composites at high strain rate. Finally, the mechanism for the deformation of the STF/Kevlar composites under impact was carefully discussed.

2. Materials and methods

2.1. Preparation of STFs and STF/Kevlar composites

The PSt-EA nanospheres were prepared by soap free emulsion polymerization. The STFs were obtained by dispersing the PSt-EA nanospheres into ethylene glycol (EG). The suspension was mixed in a ball mill grinding up to about 24 h in order to obtain a uniform distribution. In this research, different concentrations of STFs (54 vol.%, 56 vol.% and 59 vol.% for PSt-EA) were prepared.

The fabric used in the experiment was the plain-woven aramid high performance Kevlar fabrics with an areal density of around 200 g/m^2. To fabricate the STF/Kevlar composites, the STF samples were firstly diluted 1:2 with water and then mixed for 30 min in ultrasonic dispersion method to ensure the solution was well-distributed. The Kevlar fabrics were cut and soaked in the solution individually for 5 min. After the impregnation, the fabrics were dried at 40 °C to evaporate the water. The weight of Kevlar fabrics was recorded before and after the impregnation. The detail data was summarized in Table 1.

2.2. Methods

According to the NIJ standard 0115.00 (Stab Resistance of Personal Body Armor), a drop tower (Fig. 1(a)) was used to test the stab resistance of STF/Kevlar composites. An acceleration sensor was set on the drop mass to record the acceleration signal during the test. The 10 cm × 10 cm fabric targets were placed on the multi-layer foam backing as presented in Fig. 1(d). The multi-layer foam backing consists of neoprene sponge, witness paper, closed-cell polyethylene foam and rubber. During the stab resistance test, the knife or spike impactor (Fig. 1(b) and (c)) was fixed on the drop mass. The drop mass was set to 2.2 kg for knife and spike. The impactor dropped freely to impact the target from a fixed height. The impact energy of the impactor changed along with the height. The number of penetrated witness papers corresponded to the depth of penetration. So it could be used to evaluate the stab resistance of target.

Dynamic anti-impact property of the STF/Kevlar composites was tested on a typical split Hopkinson pressure bar (SHPB) system. The system mainly consists of a striker bar, an incident bar, a transmission bar, an absorber bar and an absorber (Fig. 2). All the bars are made of aluminum because of its low mechanical impedance. The elastic modulus of aluminum is 70 GPa and the density is 2700 kg/m^3. In this research, the diameter of aluminum bars is 14.5 mm. The lengths of the striker bar, the incident bar and the transmission bar are 200 mm, 1500 mm and 800 mm, respectively. To guarantee that the rising edge of the incident wave is gentle and the sample could obtain stress equilibrium, a rubber pulse shaper (1 mm × 1 mm) was placed on the front face of the incident bar. The fabric specimen was cut into a shape of regular octagon to maintain geometric similarity with the bars. The striker bar was driven by a light-gas gun and its velocity was recorded by a photoelectric door. The signals of incident bar and transmission bar were recorded by strain gages and presented on an oscilloscope.

The test of SHPB is based on the stress equilibrium assumption. Therefore, it is necessary to conform the data satisfy the assumption. As shown in Fig. 3, the shape of incident wave σ_I is close to sum of transmission wave σ_T and reflected wave σ_R. It can be concluded that:

$$\sigma_I = \sigma_R + \sigma_T \tag{1}$$

The energy contained in the stress pulse in the bars can be expressed as:

$$U = \frac{c_b A_b}{2E_b}\int_0^T \sigma^2(t)dt + \frac{\rho_b A_b c_b^3}{2E_b^2}\int_0^T \sigma^2(t)dt \tag{2}$$

where U is the energy contained in the stress pulse. c_b, A_b, E_b and ρ_b are the elastic wave speed, the cross-sectional area, the elastic modulus and the density of the bars, respectively. σ is the stress, T is the pulse length. The first term is the strain energy and the second term is the kinetic energy. The elastic wave speed c_b, the elastic modulus E_b, and the density ρ_b are found to follow a relationship as shown:

$$\rho_b = \frac{E_b}{c_b^2} \tag{3}$$

Combining Eq. (3) with Eq. (2), it is clear that

Table 1
Data of the STF-treated fabric composite.

	Neat fabric	Impregnated with EG	Impregnated with 54 vol.% STF	Impregnated with 56 vol.% STF	Impregnated with 59 vol.% STF
Areal density (g/m^2)	199	242	240	239	236
Weight addition (%)	0	22.0	21.2	20.5	18.8

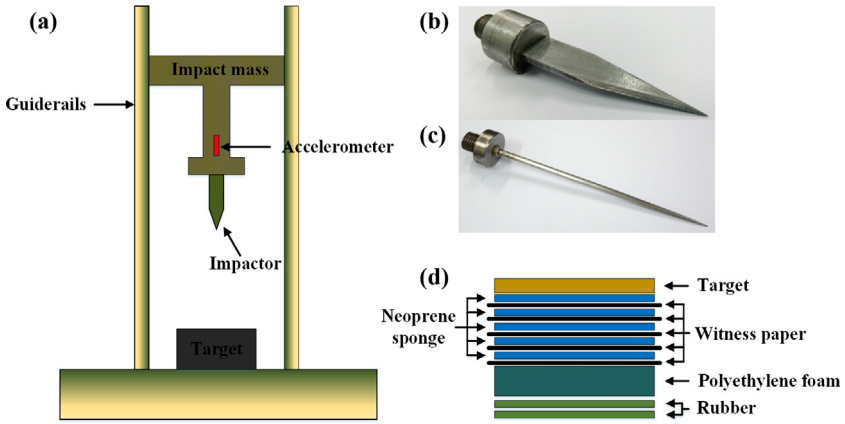

Fig. 1. (a) Schematic illustration of a drop tower. (b) Image of the knife impactor. (c) Image of the spike impactor. (d) Schematic illustration of the stab resistance test fabrics and backing material. (For interpretation of the references to color in this figure legend, the reader is referred to the web version of this article.)

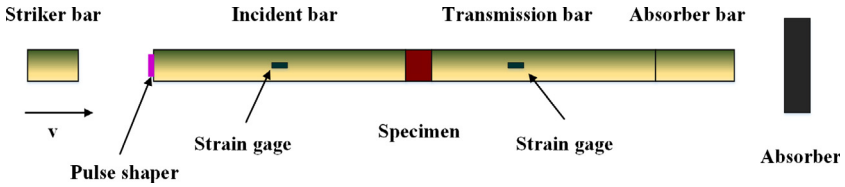

Fig. 2. Schematic illustration of a SHPB system. (For interpretation of the references to color in this figure legend, the reader is referred to the web version of this article.)

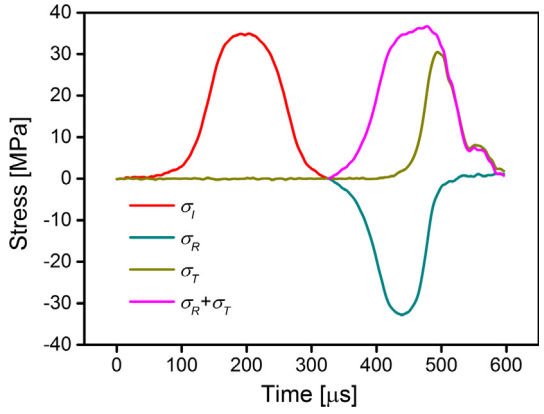

Fig. 3. The stress equilibrium assumption of SHPB test. (For interpretation of the references to color in this figure legend, the reader is referred to the web version of this article.)

$$U = \frac{c_b A_b}{E_b} \int_0^T \sigma^2(t) dt \tag{4}$$

The energy transfer rate is used to reflect the energy absorption of the fabric specimen. It can be expressed as:

$$\alpha = \frac{U_t}{U_i} \tag{5}$$

where U_t is the energy of the stress in the transmission bar and U_i is the energy of the stress in the incident bar.

According to the one-dimension stress wave propagation theory [36–43], the dynamic stress, dynamic strain and the dynamic strain rate in the sample can be expressed as:

$$\sigma_s = \frac{E_b A_b}{A_s} \varepsilon_t \tag{6}$$

$$\varepsilon_s = -\frac{2c_b}{l_s} \int_0^T (\varepsilon_i - \varepsilon_t) d\tau \tag{7}$$

$$\dot{\varepsilon}_s = -\frac{2c_b}{l_s} (\varepsilon_i - \varepsilon_t) \tag{8}$$

where ε_i and ε_t are the dynamic strain in the incident bar and transmission bar; σ_s, ε_s and $\dot{\varepsilon}_s$ are the dynamic stress, the dynamic strain and the dynamic strain rate in the specimen; A_b and A_s are the cross-sectional areas of the bar and the specimen; E_b, c_b and l_s are the elastic modulus of the aluminum bars, the elastic wave speed of the bars and the length of the specimen, respectively. The stress and strain calculated in Eqs. (6)–(8) are engineering stress and engineering strain respectively. The true stress and true strain can be obtained by Eqs. (9) and (10).

$$\varepsilon_T = -\ln(1 - \varepsilon_E) \tag{9}$$

$$\sigma_T = (1 - \varepsilon_E)\sigma_E \tag{10}$$

where ε_E and σ_E are the engineering strain and engineering stress; ε_T and σ_T are the true strain and true stress. All the stress and the strain mentioned in the following parts are the true stress and true strain.

3. Results and discussions

3.1. Characterization of STFs and the STF/Kevlar composites

The microstructure of PSt-EA nanospheres was investigated using scanning electron microscopy (SEM, Sirion 200) and transmission electron microscopy (TEM). Fig. 4(a) and (b) presents the SEM and TEM images of PSt-EA nanospheres. The microscopy of PSt-EA indicates that the nanospheres are monodisperse. The average particle size of PSt-EA is estimated to be around 340 nm. The morphological and surface characteristics of STF/Kevlar composite were determined by SEM. According to Fig. 4, the surface of STF/Kevlar fabric (Fig. 4(d) and (f)) is rougher than the neat fabric (Fig. 4(c) and (e)). The SEM images of STF/Kevlar fabric presented in Fig. 4(d) and (f) show that the STFs are well distributed on the surface of the yarns and part of them is located within the spaces between the fabric yarns.

3.2. Rheological properties of STFs

The rheological measurements of STF samples were conducted by a stress and strain controlled rheometer (Anton-Paar MCR 301) with cone-plate geometry (25 mm in diameter and 2° in cone angle). All the experiments were conducted with a gap size of 0.05 mm at a room temperature of 25 °C. The volume fraction of STF has a significant influence on the shear thickening effect. Fig. 5 shows the typical rheological behavior of the STF. As the volume fraction increases from 54%, 56% to 59%, the critical shear rate decreases from 289 s^{-1}, 63 s^{-1} to 19 s^{-1} and the maximum viscosity increases from 139 Pa s, 462 Pa s to 1496 Pa s, respectively. The shear thickening effects of the suspensions are strengthened with the increasing volume fraction.

3.3. Drop tower test

Stab resistance of the neat Kevlar fabrics and STF/Kevlar composites targets with a thickness of 15 layers against the knife impactor is shown in Fig. 6(a). In this test, the drop height of knife impactor varies from 0.2 m to 1.0 m. With increasing of drop height, the penetration depth increases gradually. In comparison to the neat Kevlar fabric and EG/Kevlar fabric, the STF/Kevlar presents lower penetration depth. As the volume fraction of STF increases from 54% to 59%, the penetration depth decreases from 5 layers to 4 layers at a drop height of 1.0 m. The higher volume fraction of STF shows better knife stab resistance performance for

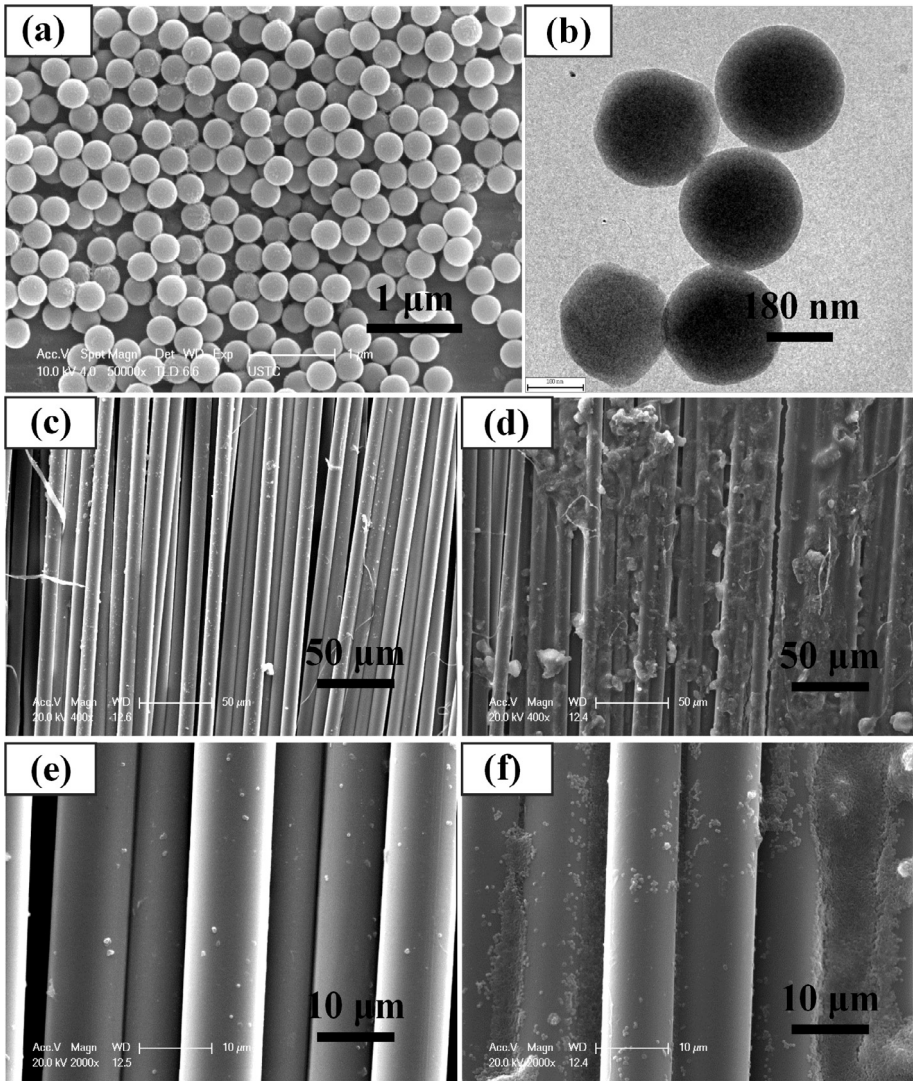

Fig. 4. SEM (a) and TEM (b) images of PSt-EA spherical particles. SEM images of neat fabric and STF-treated fabric under different magnifications: (c) neat Kevlar fabric (400×), (d) STF/Kevlar composite (400×), (e) neat Kevlar fabric (2000×), (f) STF/Kevlar composite (2000×).

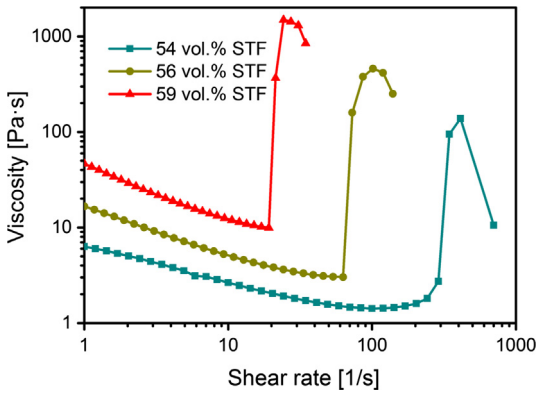

Fig. 5. Steady shear test of PSt-EA suspensions for different volume fractions: 54%, 56% and 59%. (For interpretation of the references to color in this figure legend, the reader is referred to the web version of this article.)

the STF/Kevlar composites. During the penetration process, shear stress arises from the slippage between fabrics, then the viscosity of STF increases. Higher viscosity accounts for larger friction, which prevents fabric yarns from slipping. Remarkably, EG/Kevlar shows worse knife stab resistance performance than neat Kevlar, because fluid lubrication could reduce friction between fabrics. Fig. 6(b) presents the impact force-displacement curve of the 56% STF/Kevlar sample under knife stab resistance test. Both the peak force and the maximum displacement increase with the drop height. The area enclosed by the curve and the coordinate axis represents the dissipation energy. The dissipation energy can be calculated by integrating the force-displacement curve. Therefore, it can be inferred qualitatively that the dissipation energy increases with the drop height.

The spike stab resistance test shows similar variation trend (Fig. 6(c) and (d)). The penetration depth under the spike stab resistance test at a drop height of 1.0 m is 9 layers which is much larger than the knife stab resistance test. Besides, the penetration depth of the STF/Kevlar is nearly half for that of the control group. Compared to the results presented in Fig. 6(b), the residual displacement of the spike stab resistance test is much larger because of the weaker rebound of spike impactor. The cross-sectional area of spike impactor is smaller than knife impactor. So the bearing area of target is smaller, which contributes to deeper penetration depth and lower peak force. SEM images of STF/Kevlar target after drop tower test are shown in Fig. 7. A hole is found in the target after spike stab resistance test while there is only a cut mark after knife stab resistance test. When the spike comes into contact with the fabric surface, the yarn slips and curves, resulting in a hole in the fabric. As shown in Fig. 7(a), only a few yarns are cut off for the spike stab. However, when the knife touches the surface of the fabric, the stress concentration occurs where the yarn is in contact with the blade, causing the half of yarns cluster to be cut off (Fig. 7(b)). Therefore, the failure of fabric under the spike stab resistance test is mainly due to the slippage between the fiber yarns, and the one under the knife stab resistance test is mainly attributable to the cutting-off of the fiber yarns.

3.4. SHPB test

Fig. 8(a) presents the relationship between energy transfer rate and impact velocity as well as the number of fabric specimen layer. The fabrics were impregnated with 56 vol.% STF. As the number of fabric layers increases, the energy transfer rate α decreases from 0.85 to 0.01. Remarkably, when the number of fabric layers is less than 4 layers, α decreases linearly with the number of fabric layers.

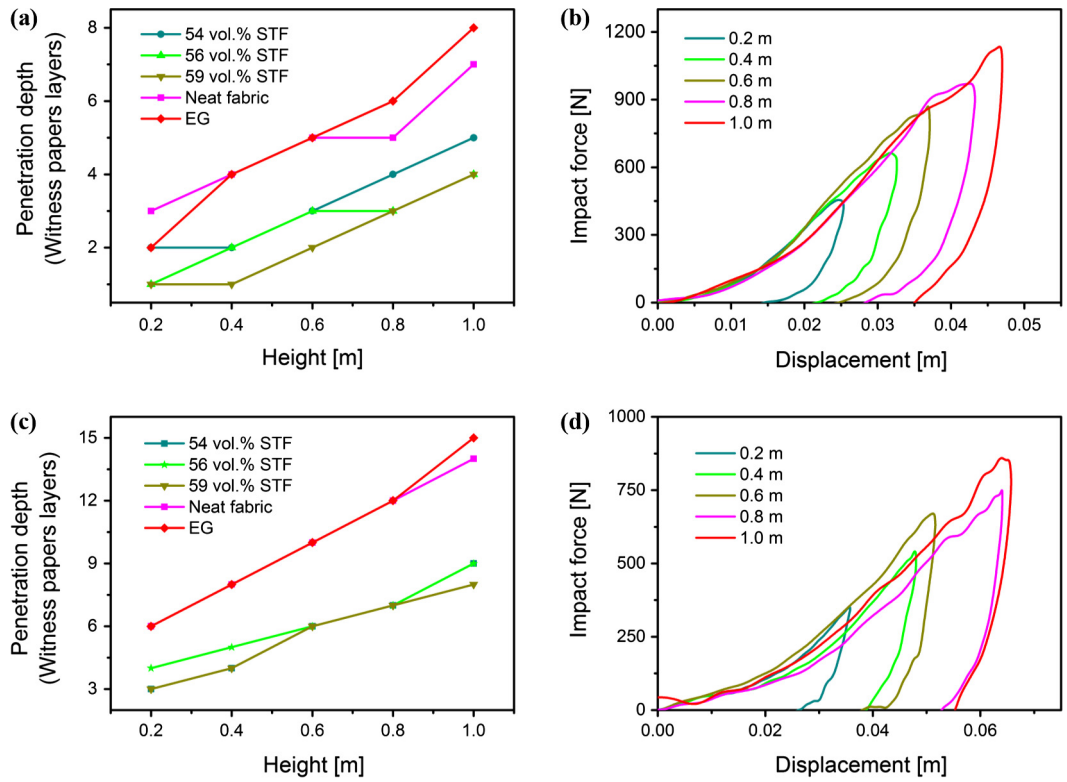

Fig. 6. Drop tower results for neat fabric, EG/Kevlar fabric and different volume fractions of STFs treated fabric from different drop heights. (a) Knife stab resistance test. (c) Spike stab resistance test. Impact force vs. displacement curve of the fabric sample treated with 56 vol.% STF under knife (b) and spike (d) stab resistance test. (For interpretation of the references to color in this figure legend, the reader is referred to the web version of this article.)

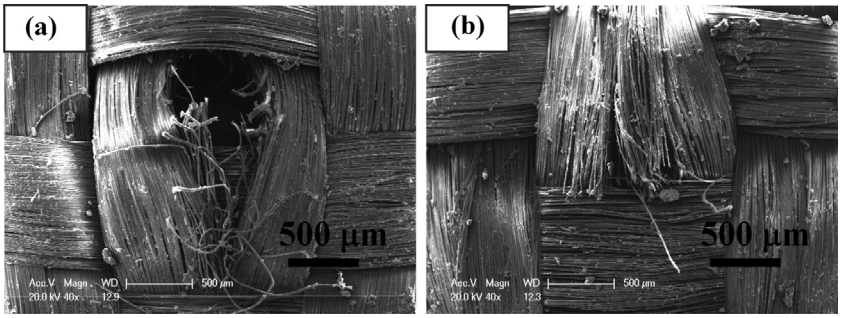

Fig. 7. SEM images of the fabric impregnated with 56 vol.% STF after drop tower: (a) the spike impactor; (b) the knife impactor.

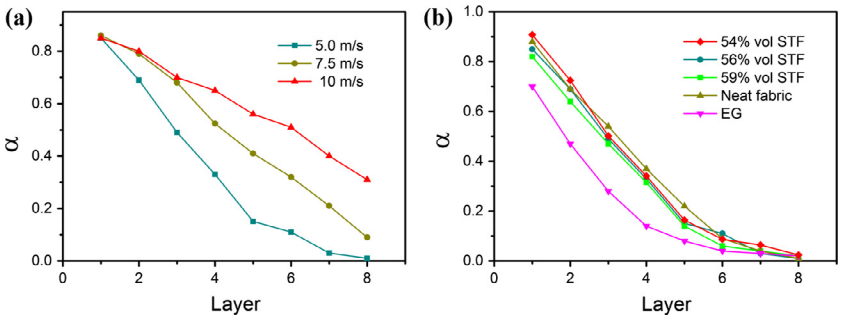

Fig. 8. (a) The energy transfer rate versus the number of fabric layers and the impact velocity. The fabrics were impregnated with 56 vol.% STF. (b) The energy transfer rate versus different kinds of fabrics. The impact velocity was 5 m/s. (For interpretation of the references to color in this figure legend, the reader is referred to the web version of this article.)

However, α becomes insensitive to the number of fabric layers as the number of fabric layers exceeds 4 layers. With the increase of impact velocity, α also shows an increasing trend. The results of fabrics impregnated with different volume fractions of STF are shown in Fig. 8(b). The neat Kevlar fabric and the EG/Kevlar fabric were tested as comparison. The number of fabric layers in each group was 4 layers and the impact velocity was 5 m/s. The value of α in five groups performs a similar change trend. Although the EG/Kevlar fabric exhibits the minimum energy transfer rate, its weaving structure is broken during the impact. It can't prevent bullets from transferring through the body and can't continue to provide protection. In addition to the poorest stab resistance property, the EG/Kevlar fabric can't be the optimal choice of body armor. From Fig. 8(b), the energy transfer rate of STF treated fabrics are identical with the neat fabric. The fabric impregnated with 59 vol.% STF shows the lower energy transfer rate than the 54 vol.% and 56 vol.% STF. Considering the results of weight addition (Table 1), the impregnation of STF with high volume fraction into the fabric can not only reduce weight but also enhance the energy absorption.

Fig. 9(a) presents the stress-stain curve for different layers of fabrics at a velocity of 5 m/s. The fabrics were impregnated with 56 vol.% STF and the number of fabrics varied from 2 layers to 8 layers. With increasing the fabric layers, the maximum stress in the fabric specimen decreases from 23.3 MPa to 3.7 MPa. This means that there is a significant dissipation in the fabrics under the impact. The modulus of the fabric specimen can be calculated from the slope of the stress-strain curve. It can reflect the slippage of the fabric yarns. The modulus and strain rate involved in the following are the maximum strain rate and the maximum modulus. The strain rate and modulus calculated from the stress-strain curve are presented in Fig. 9(b). With the increase of the fabric layers, both the strain rate and the modulus show a decreasing trend. As the thickness of the fabric specimen increases, the propagation time of the stress wave in the fabric specimen becomes longer and therefore the strain rate decreases. The modulus of the fabric specimen subjected to impact is related to the strain rate, which reflects the property of the viscoelastic material.

Impact velocity has a great effect on the dynamic mechanical properties of the fabrics. Fig. 9(c) shows the stress-strain curves of the 4-layer fabric samples impregnated with 56 vol.% STF by varying the impact velocities from 5 m/s to 7.5 m/s and 10 m/s, respectively. During the impact process, the fiber specimen first undergoes an elastic section which shows a flat curve. The elastic section of the fabric specimen is independent on the strain rate, so the initial sections of the three stress-strain curves are almost coincident. Then, the plastic deformation arises in the fabric specimen, in which the fiber specimen exhibits a strain rate stiffening character (Fig. 9(d)). As the impact velocity increases, the strain rate of the fabric specimen varies from 4318 s^{-1}, 6438 s^{-1} to 8702 s^{-1} and the modulus also increases from 239 MPa, 386 MPa to 490 MPa, respectively. The modulus and strain rate show a positive correlation.

In order to study the effect of volume fraction of STF on the dynamic mechanical properties of fabric samples, 3 groups of fabric specimens impregnated with different volume fractions of STF were tested. The neat Kevlar fabric and the EG/Kevlar fabric were also tested as comparison. The number of fabrics was 4 layers and the impact velocity was 5 m/s. From the results shown in Fig. 9(e) and (f), it is found that the strain rates of five kinds of fabrics are relatively close. But the modulus of the fabrics are significantly different. The modulus of neat Kevlar and EG/Kevlar are close to 155 MPa. But the modulus of STF/Kevlar composite increases from 188 MPa, 239 MPa to 247 MPa as the volume fraction of STF varies from 54%, 56% to 59%. The addition of STF significantly increases the modulus of the fabrics. It is worth noting that the stress-strain curve of the EG/Kevlar is different from other groups. The stress-strain curve shows that the EG/Kevlar reaches

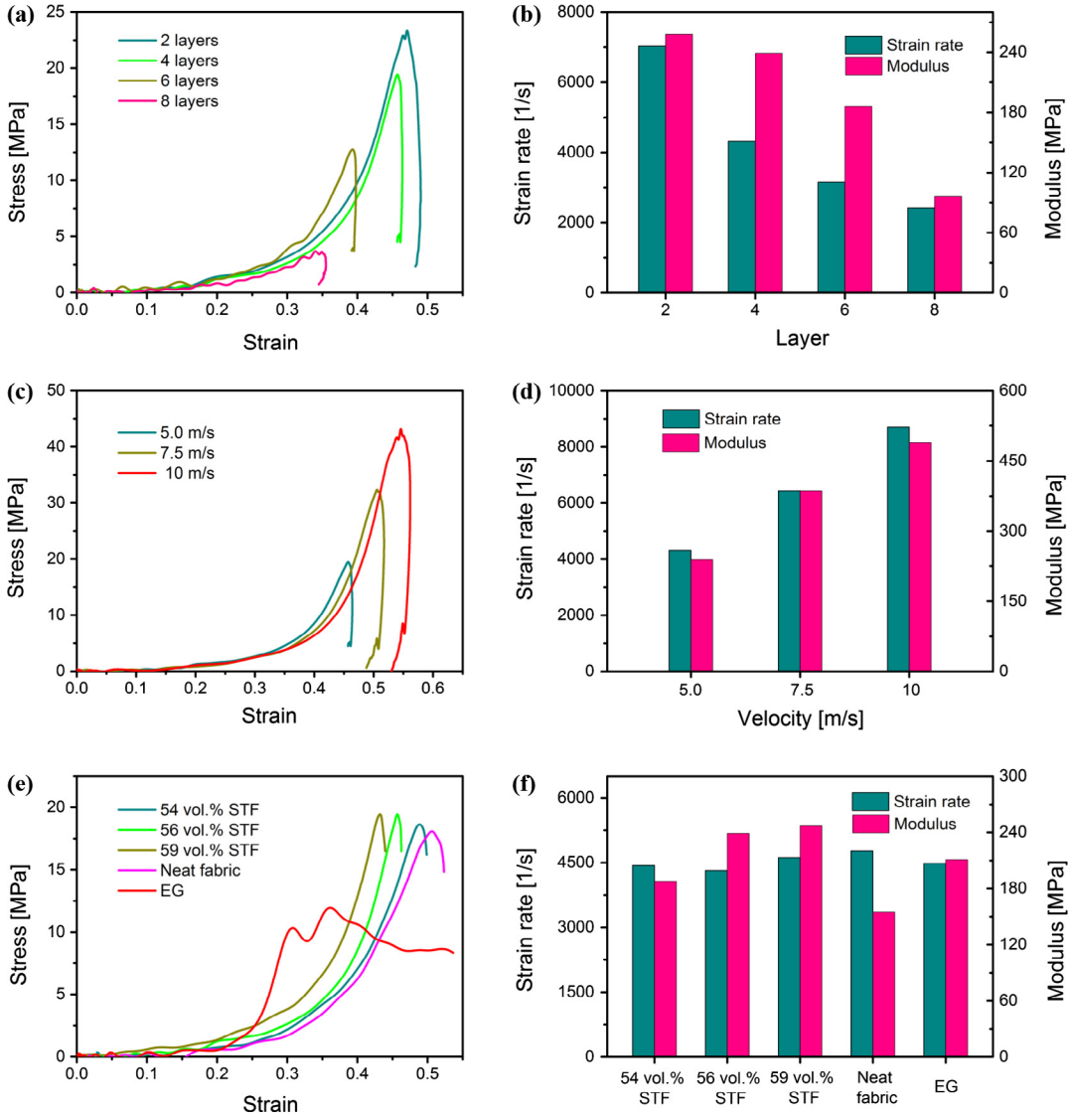

Fig. 9. Stress-strain curves of the fabric specimen and the results of strain rate and modulus under different SHPB test conditions: (a) and (b) different number of fabric layers, the fabrics were impregnated with 56 vol.% and the velocity was 5 m/s; (c) and (d) different velocities, the fabrics were impregnated with 56 vol.% STF and the fabrics were prepared with 4 layers; (e) and (f) different kinds of fabrics, the fabrics were prepared with 4 layers and the velocity was 5 m/s. (For interpretation of the references to color in this figure legend, the reader is referred to the web version of this article.)

yield stress and the structure is destroyed after impact. However, only plastic deformation in the fabrics of other groups is found in Fig. 10. The morphologies of the neat Kevlar, the EG/Kevlar and the STF/Kevlar composite before impact are similar (Fig. 10(a)). After impact, the weaving structure of the EG/Kevlar is damaged (Fig. 10(d)), whereas the neat Kevlar and the STF/Kevlar composite have not changed significantly (Fig. 10(b) and (c)). Due to limitations of the experimental conditions, the neat Kevlar and the STF/Kevlar composite do not reach the yield stress and failure in our present progress. Further work will be done to investigate the detailed yield process. Fortunately, because of the strength and high friction of fibers [17–20], the STF/Kevlar composite exhibits a good potential of energy absorption. Fig. 10(e) and (f) shows the cross-sectional topography of the fabric clusters before and after impact. Before the impact, the fabric clusters are elliptical in cross-section and the fabric yarns inside the fabric clusters are looser. After the impact, the cross-section of the fabric clusters becomes a more flat ellipse and the arrangement of the fabric yarns is more compact.

A schematic diagram is put forward to explain the structural evolution of fabrics in the SHPB test. When subjected to impact, the fabric first undergoes a process of elastic compaction of a woven structure. This phenomenon is corresponding to the section I in Fig. 11. The elastic section of the fabric specimen is independent of the strain rate, so the initial sections of the stress-strain curves are similar. Then the plastic deformation arises in the fabric specimen. In section II, the fabric yarns slide and the gap between the yarns is reduced. STF is a type of non-newton fluid. When the shear rate exceeds a critical value, the viscosity of STF increases dramatically. During the SHPB test, the STF is in a shear thickening (ST) state since the impact strain rate is higher than the critical shear rate. The STF around the yarns increases the friction between the yarns and thereby prevents the yarn from slipping. At this time, the fabric composite exhibits strain rate stiffening. In section III, the fabric yarns are crushed and the gap between the yarns is further reduced. The modulus of the fabric increases with the increase of the strain rate. However, under the same strain rate, the modulus of the fabric increases with the increase of the volume fraction

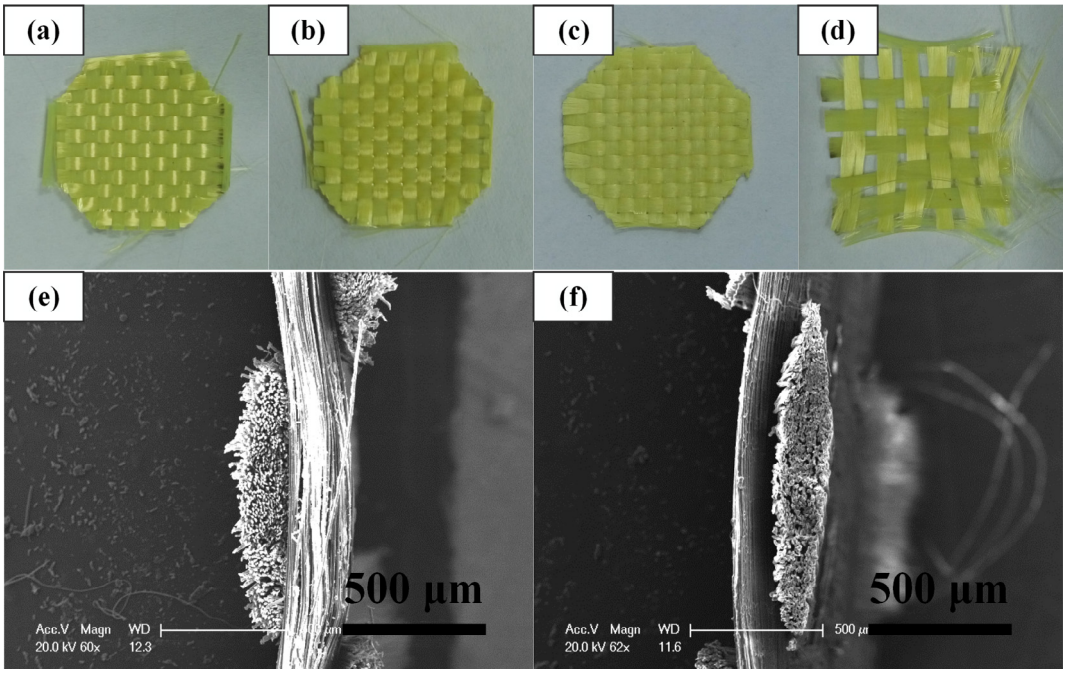

Fig. 10. Images of fabric samples before and after impact: (a) the neat Kevlar fabric before impact; (b) the neat Kevlar fabric after impact; (c) the STF/Kevlar composite after impact, the volume fraction of STF is 59%; (d) the EG/Kevlar fabric after impact. SEM images of the cross-section of the STF/Kevlar composite before (e) and after (f) impact, the volume fraction of STF is 59%. (For interpretation of the references to color in this figure legend, the reader is referred to the web version of this article.)

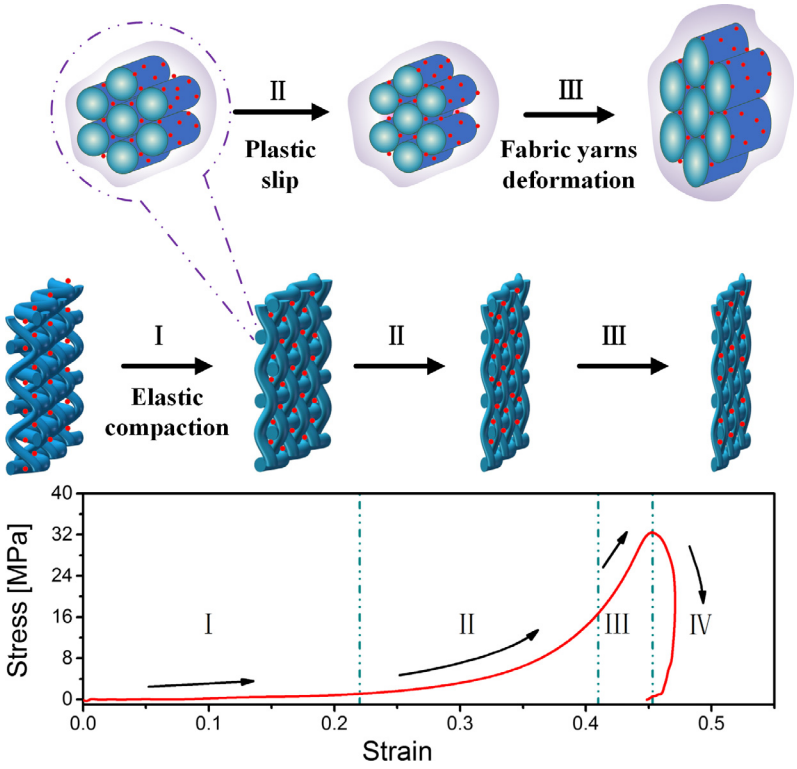

Fig. 11. Schematic diagram of the structural evolution of fabric under the SHPB test. The stress-strain curve is divided into four sections. Section I: Elastic compaction of the weaving structure. Section II: Plastic slip of the fabric yarns. Section III: Deformation of the fabric yarns. Section IV: Stress unloading of the fabric specimen. (For interpretation of the references to color in this figure legend, the reader is referred to the web version of this article.)

of STF, which must be attributed to the increasing shear thickening effects. Section IV is the unloading area. The fabric exhibits a viscoelastic character. The stress in the fabric decreases while the strain continues to increase.

4. Conclusions

In this article, the stab resistance performance and the dynamic mechanical properties of the STF/Kevlar composite were investi-

gated. The STF enhanced the friction between fabric yarns due to its high viscosity under shear. The slippage of fabric yarns was reduced and the stab resistance of fabric got significant enhancement. During the SHPB test, both the strain rate and the modulus of the STF/Kevlar composite showed an increasing trend with the increase of impact velocity. Besides, the modulus of composite increased with the increasing of the volume fraction of STF. The addition of the STF and the increase of the fabric number reduced the energy transfer rate. The energy absorption of the STF/Kevlar increased with the volume fraction of the STF. It could be speculated that multilayer fabrics impregnated with high volume fraction of STF was the optimal choice for energy absorption.

Acknowledgements

Financial supports from the National Natural Science Foundation of China (Grant No. 11372301), the Fundamental Research Funds for the Central Universities (WK2480000002), and the Strategic Priority Research Program of the Chinese Academy of Sciences (Grant No. XDB22040502) are gratefully acknowledged. This work was also supported by Collaborative Innovation Center of Suzhou Nano Science and Technology.

References

[1] Jacobs MJN, Van Dingenen JLJ. Ballistic protection mechanisms in personal armour. J Mater Sci 2001;36(13):3137–42.
[2] Zhang GM, Batra RC, Zheng J. Effect of frame size, frame type, and clamping pressure on the ballistic performance of soft body armor. Compos B – Eng 2008;39(3):476–89.
[3] Dong Z, Sun CT. Testing and modeling of yarn pull-out in plain woven Kevlar fabrics. Compos A – Appl Sci Manuf 2009;40(12):1863–9.
[4] Barnes HA. Shear-thickening (Dilatancy) in suspensions of nonaggregating solid particles dispersed in newtonian liquids. J Rheol 1989;33(2):329–66.
[5] Laun HM, Bung R, Schmidt F. Rheology of extremely shear thickening polymer dispersions (passively viscosity switching fluids). J Rheol 1991;35(6):999–1034.
[6] Zhang XZ, Li WH, Gong XL. Study on magnetorheological shear thickening fluid. Smart Mater Struct 2008;17(1):015051.
[7] Ye F, Zhu W, Jiang WQ, Wang ZY, Chen Q, Gong XL, et al. Influence of surfactants on shear-thickening behavior in concentrated polymer dispersions. J Nanopart Res 2013;15(12):2122.
[8] Tan ZH, Zuo L, Li WH, Liu LS, Zhai PC. Dynamic response of symmetrical and asymmetrical sandwich plates with shear thickening fluid core subjected to penetration loading. Mater Des 2016;94:105–10.
[9] Decker MJ, Halbach CJ, Nam CH, Wagner NJ, Wetzel ED. Stab resistance of shear thickening fluid (STF)-treated fabrics. Compos Sci Technol 2007;67(3–4):565–78.
[10] Hassan TA, Rangari VK, Jeelani S. Synthesis, processing and characterization of shear thickening fluid (STF) impregnated fabric composites. Mater Sci Eng A-Struct 2010;527(12):2892–9.
[11] Kang TJ, Hong KH, Yoo MR. Preparation and properties of fumed silica/Kevlar composite fabrics for application of stab resistant material. Fiber Polym 2010;11(5):719–24.
[12] Yu KJ, Cao HJ, Qian K, Jiang LL, Li HS. Synthesis and stab resistance of shear thickening fluid (STF) impregnated glass fabric composites. Fibres Text East Eur 2012;20(6A):126–8.
[13] Majumdar A, Butola BS, Srivastava A. An analysis of deformation and energy absorption modes of shear thickening fluid treated Kevlar fabrics as soft body armour materials. Mater Des 2013;51:148–53.
[14] Sun LL, Xiong DS, Xu CY. Application of shear thickening fluid in ultra high molecular weight polyethylene fabric. J Appl Polym Sci 2013;129(4):1922–8.
[15] Feng XY, Li SK, Wang Y, Wang YC, Liu JX. Effects of different silica particles on quasi-static stab resistant properties of fabrics impregnated with shear thickening fluids. Mater Des 2014;64:456–61.
[16] Firouzi D, Foucher DA, Bougherara H. Nylon-coated ultra high molecular weight polyethylene fabric for enhanced penetration resistance. J Appl Polym Sci 2014;131(11):169–72.
[17] Gong XL, Xu YL, Zhu W, Xuan SH, Jiang WF, Jiang WQ. Study of the knife stab and puncture-resistant performance for shear thickening fluid enhanced fabric. J Compos Mater 2014;48(6):641–57.
[18] Hasanzadeh M, Mottaghitalab V. The role of shear-thickening fluids (STFs) in ballistic and stab-resistance improvement of flexible armor. J Mater Eng Perform 2014;23(4):1182–96.
[19] Li W, Xiong DS, Zhao XD, Sun LL, Liu J. Dynamic stab resistance of ultra-high molecular weight polyethylene fabric impregnated with shear thickening fluid. Mater Des 2016;102:162–7.
[20] Gürgen S, Kuşhan MC. The stab resistance of fabrics impregnated with shear thickening fluids including various particle size of additives. Compos A – Appl Sci Manuf 2017;94:50–60.
[21] Kalman DP, Merrill RL, Wagner NJ, Wetzel ED. Effect of particle hardness on the penetration behavior of fabrics intercalated with dry particles and concentrated particle-fluid suspensions. ACS Appl Mater Interfaces 2009;1(11):2602–12.
[22] Bilisik K. Properties of yarn pull-out in para-aramid fabric structure and analysis by statistical model. Compos A – Appl Sci Manuf 2011;42(12):1930–42.
[23] Zhu D, Soranakom C, Mobasher B, Rajan SD. Experimental study and modeling of single yarn pull-out behavior of kevlar® 49 fabric. Compos A – Appl Sci Manuf 2011;42(7):868–79.
[24] Hasanzadeh M, Mottaghitalab V, Babaei H, Rezaei M. The influence of carbon nanotubes on quasi-static puncture resistance and yarn pull-out behavior of shear-thickening fluids (STFs) impregnated woven fabrics. Compos A – Appl Sci Manuf 2016;88:263–71.
[25] Lee YS, Wetzel ED, Wagner NJ. The ballistic impact characteristics of Kevlar (R) woven fabrics impregnated with a colloidal shear thickening fluid. J Mater Sci 2003;38(13):2825–33.
[26] Kang TJ, Kim CY, Hong KH. Rheological behavior of concentrated silica suspension and its application to soft armor. J Appl Polym Sci 2012;124(2):1534–41.
[27] Kordani N, Vanini AS. Optimizing the ethanol content of shear thickening fluid/fabric composites under impact loading. J Mech Sci Technol 2014;28(2):663–7.
[28] Park Y, Kim Y, Baluch AH, Kim CG. Empirical study of the high velocity impact energy absorption characteristics of shear thickening fluid (STF) impregnated Kevlar fabric. Int J Impact Eng 2014;72:67–74.
[29] Haro EE, Szpunar JA, Odeshi AG. Ballistic impact response of laminated hybrid materials made of 5086-H32 aluminum alloy, epoxy and Kevlar (R) fabrics impregnated with shear thickening fluid. Compos A – Appl Sci Manuf 2016;87:54–65.
[30] Lu ZQ, Jing XY, Sun BZ, Gu BH. Compressive behaviors of warp-knitted spacer fabrics impregnated with shear thickening fluid. Compos Sci Technol 2013;88:184–9.
[31] Haris A, Lee HP, Tay TE, Tan VBC. Shear thickening fluid impregnated ballistic fabric composites for shock wave mitigation. Int J Impact Eng 2015;80:143–51.
[32] Na W, Ahn H, Han S, Harrison P, Park JK, Jeong E, et al. Shear behavior of a shear thickening fluid-impregnated aramid fabrics at high shear rate. Compos B – Eng 2016;97:162–75.
[33] Lu ZQ, Wu LW, Gu BH, Sun BZ. Numerical simulation of the impact behaviors of shear thickening fluid impregnated warp-knitted spacer fabric. Compos B – Eng 2015;69:191–200.
[34] Park Y, Kim Y, Baluch AH, Kim CG. Numerical simulation and empirical comparison of the high velocity impact of STF impregnated Kevlar fabric using friction effects. Compos Struct 2015;125:520–9.
[35] Lee BW, Kim CG. Computational analysis of shear thickening fluid impregnated fabrics subjected to ballistic impacts. Adv Compos Mater 2012;21(2):177–92.
[36] Wu XF, Ghoshal G, Kartashov M, Aslan Z, Turner JA, Dzenis YA. Experimental characterization of the impact-damage tolerance of a cross-ply graphite-fiber/epoxy laminate. Polym Compos 2008;29(5):534–43.
[37] Lim AS, Lopatnikov SL, Wagner NJ, Gillespie JW. Investigating the transient response of a shear thickening fluid using the split Hopkinson pressure bar technique. Rheol Acta 2010;49(8):879–90.
[38] Lim AS, Lopatnikov SL, Wagner NJ, Gillespie JW. An experimental investigation into the kinematics of a concentrated hard-sphere colloidal suspension during Hopkinson bar evaluation at high stresses. J Non-Newton Fluid 2010;165(19–20):1342–50.
[39] Lomakin EV, Mossakovsky PA, Bragov AM, Lomunov AK, Konstantinov AY, Kolotnikov ME, et al. Investigation of impact resistance of multilayered woven composite barrier impregnated with the shear thickening fluid. Arch Appl Mech 2011;81(12):2007–20.
[40] Jiang WF, Gong XL, Xuan SH, Jiang WQ, Ye F, Li XF, et al. Stress pulse attenuation in shear thickening fluid. Appl Phys Lett 2013;102(10):101901.
[41] Liao GJ, Gong XL, Xuan SH. Magnetic field-induced compressive property of magnetorheological elastomer under high strain rate. Ind Eng Chem Res 2013;52(25):8445–53.
[42] Woo SC, Kim TW. High-strain-rate impact in Kevlar-woven composites and fracture analysis using acoustic emission. Compos B – Eng 2014;60:125–36.
[43] Wang YP, Wang S, Xu CH, Xuan SH, Jiang WQ, Gong XL. Dynamic behavior of magnetically responsive shear-stiffening gel under high strain rate. Compos Sci Technol 2016;127:169–76.
[44] Parmley LF, Manion WC, Mattingly TW. Nonpenetrating traumatic injury of the heart. Circulation 1958;18(3):371–96.
[45] Roberts JC, Merkle AC, Biermann PJ, Ward EE, Carkhuff BG, Cain RP, et al. Computational and experimental models of the human torso for non-penetrating ballistic impact. J Biomech 2007;40(1):125–36.
[46] Roberts JC, O'connor JV, Ward EE. Modeling the effect of nonpenetrating ballistic impact as a means of detecting behind-armor blunt trauma. J Trauma Acute Care Surg 2005;58(6):1241–51.